Human Pancreatic Lipase: Colipase Dependence and Interfacial Binding of Lid Domain Mutants†

Sofiane Bezzine, Francine Ferrato, Margarita G. Ivanova, Véronique Lopez, Robert Verger, and Frédéric Carrière*

Laboratoire de Lipolyse Enzymatique, CNRS-IFR1, UPR 9025, 31 chemin Joseph Aiguier, 13402 Marseille Cedex 20, France

Received November 2, 1998; Revised Manuscript Received January 20, 1999

ABSTRACT: Five key amino acid residues from human pancreatic lipase (HPL) are mutated in some pancreatic lipase-related proteins 2 (PLRP2) that are not reactivated by colipase in the presence of bile salts. One of these residues (Y403) is involved in a direct interaction between the HPL C-terminal domain and colipase. The other four residues (R256, D257, Y267, and K268) are involved in the interactions stabilizing the open conformation of the lid domain, which also interacts with colipase. Here we produced and characterized three HPL mutants: HPL Y403N, an HPL four-site mutant (R256G, D257G, Y267F, and K268E), and an HPL five-site mutant (R256G, D257G, Y267F, K268E, and Y403N), in which the HPL amino acids were replaced by those present in human PLRP2. Colipase reactivated both the HPL Y403N mutant and HPL, and Y403 is therefore not essential for lipase−colipase interactions. Both the HPL four-site and five-site mutants showed low activity on trioctanoin, were inhibited by bile salts (sodium taurodeoxycholate, NaTDC) and were not reactivated by colipase. The interfacial binding of the HPL four-site mutant to a trioctanoin emulsion was suppressed in the presence of 4 mM NaTDC and was not restored by addition of colipase. Protein blotting/protein overlay immunoassay revealed that the HPL four-site mutant−colipase interactions are not abolished, and therefore, the absence of reactivation of the HPL four-site mutant is probably due to a lid domain conformation that prevents the interfacial binding of the lipase−colipase complex. The effects of colipase were also studied with HPL(−lid), an HPL mutant showing an 18-residue deletion within the lid domain, which therefore has only one colipase interaction site. HPL(−lid) showed a low activity on trioctanoin, was inhibited by bile salts, and recovered its lipase activity in the presence of colipase. Reactivation of HPL(−lid) by colipase was associated with a strong interfacial binding of the mutant to a trioctanoin emulsion. The lid domain is therefore not essential for either the interfacial binding of HPL or the lipase−colipase interactions.

Human pancreatic lipase (HPL) alone is inactive in vitro on an emulsified triglyceride substrate in the presence of supramicellar concentrations of bile salts such as those found in the small intestine. Bile salts are amphiphilic molecules that bind to the oil−water interface and prevent pancreatic lipase adsorption, and thus lipolysis, from occurring (*1, 2*). The inhibition by bile salts can, however, be reversed by the specific pancreatic lipase cofactor colipase (*1, 3*−*5*), via the formation of a specific 1:1 lipase−colipase complex (*6*).

The structures of the HPL−porcine procolipase complex have shown how the colipase anchors the lipase to an interface in the presence of bile salts (*7, 8*). Colipase is an amphiphilic protein with a "three finger" topology comparable to that of snake toxins (*7, 9*). The tips of the fingers contain most of the hydrophobic amino acids and form the interfacial binding site. Colipase binds to the noncatalytic C-terminal domain of pancreatic lipase and exposes the hydrophobic tips of its fingers at the opposite side of its lipase-binding site. These hydrophobic tips probably help to bring the catalytic N-terminal domain of pancreatic lipase into close contact with the interface, where a drastic change occurs in the conformation of the lid domain, a surface loop controlling the access of substrate to the active site. As the result of this structural reorganization, the N-terminal part of colipase binds to the lid domain, thus forming a second lipase−colipase interaction site. The open lid and the extremities of the colipase fingers, as well as the β9 loop (*10*), form an impressive continuous hydrophobic plateau extending over more than 50 Å, which might be able to interact strongly with a lipid/water interface. All these events are schematically depicted in Figure 1.

On the basis of recent neutron diffraction data obtained with the porcine pancreatic lipase−colipase−tetra(ethylene glycol) monooctyl ether complex, it was recently proposed by Hermoso et al. (*11*) that the activation of pancreatic lipase is not interfacial under in vivo conditions and that the opening of the lid domain may occur in "solution" via the formation of a specific ternary complex including lipase, colipase, and a bile salt micelle. Hermoso et al. stated that colipase and the distal part of the lipase C-terminal domain were the exclusive sites for interaction with a detergent micelle in their crystal structure. In the structural study at 2.46 Å resolution of the open lipase/colipase complex by Egloff et al. (*12*), several nonionic detergent molecules (β-octyl glucoside) were, however, clearly observed along the extended hydro-

† This research was carried out with financial support of the BIOTECH G programs of the European Union under Contracts BIO2-CT94-3013 and BIO2-CT94-3041.

* Corresponding author: Tel (33) 491 16 41 92; Fax (33) 491 71 58 57; Email carriere@ibsm.cnrs-mrs.fr.

10.1021/bi982601x CCC: $18.00
Published on Web 04/09/1999

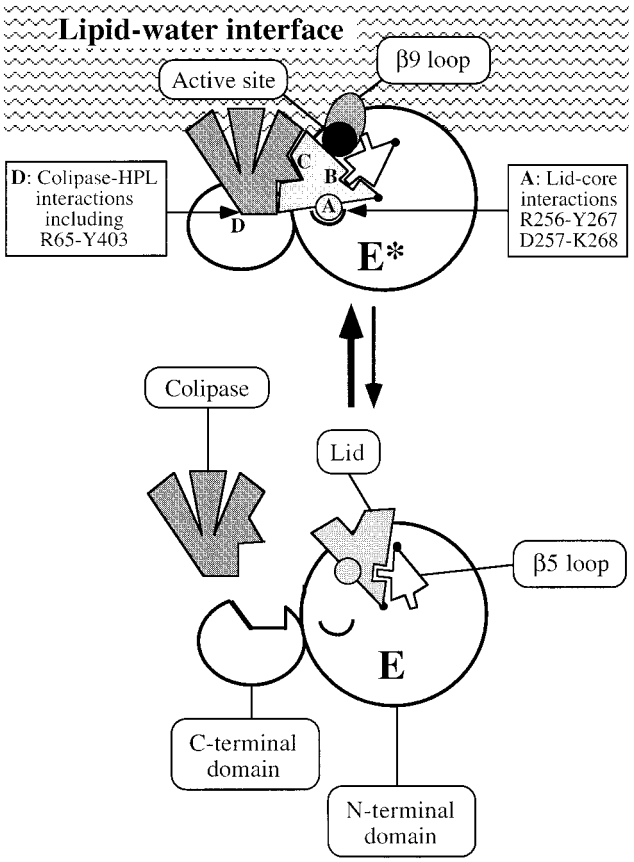

FIGURE 1: Diagram of the pancreatic lipase−colipase interactions and adsorption of the complex at a lipid−water interface. E and E* denote the pancreatic lipase in the bulk phase and the interface, respectively. The capital letters indicate the interactions between the lid domain and the protein core (A), the lid domain and the β5 loop (B), the lid domain and colipase (C), and the lipase C-terminal domain and colipase (D). Upon the opening of the lid domain, the β5 loop also changes its conformation, forming the oxyanion hole, and the hydrophobic β9 loop is unmasked.

phobic plateau consisting of the lid domain, the β9 loop, and the hydrophobic tips of colipase, thus mimicking the interaction between the lipase−colipase complex and the lipid/water interface.

Colipase interacts with the C-terminal domain of pancreatic lipase, mainly via polar interactions (two salt bridges and six hydrogen bonds), but the stacking of the R65 guanidinium group from colipase with the Y403 aromatic ring from lipase might be one of the main components of the apolar interaction between lipase and colipase (*7*, *13*). The surface involved in the interaction between the pancreatic lipase C-terminal domain and colipase is 612 Å^2 in size. Upon the opening of the lid domain, three additional hydrogen bonds and several van der Waals contacts are formed between N240, S243, and V246 from lipase and E15, L16, and R38 from colipase. The total surface of interaction between lipase and colipase increases up to 950 Å^2 (+338 Å^2). The affinity of lipase and colipase has been reported to be low in solution [$(1-2) \times 10^6$ M^{-1} (*6*, *14*)] but to increase by several orders of magnitude in the presence of lipids or amphiphiles [$2 \times 10^7 - 1 \times 10^9$ M^{-1} (*15*−*18*)]. It is difficult, however, to determine what the intrinsic affinities may be because the constants mentioned above were determined in a heterogeneous system and are therefore only apparent values (*19*).

Several novel pancreatic lipases have been isolated from mammals during recent years, and the pancreatic lipase family now falls into three subgroups with roughly 70% amino acid identity: (i) classical pancreatic lipases, (ii) pancreatic lipase-related proteins 1 (PLRP1), and (iii) pancreatic lipase-related proteins 2 (PLRP2) (*20*). This classification was further justified by the biochemical characterization of these novel proteins (*21*, *22*). All the PLRP2s characterized to date show atypical enzymatic behavior in comparison with the classical pancreatic lipases. They display not only triacylglycerol lipase activity but also phospholipase A_1 and galactolipase activities. In addition, it has been demonstrated with trioctanoin as substrate that colipase does not reactivate the lipase activity of the PLRP2s from guinea pig (GPLRP2) or coypu (CoPLRP2) in the presence of bile salts above their critical micellar concentration (cmc) (*21*).

The lack of colipase effect on GPLRP2 probably results from several key mutations: among the 12 residues in the HPL C-terminal domain involved in colipase binding, nine differ in GPLRP2 (*23*). Moreover, no interaction between colipase and the lid domain can occur because GPLRP2 possesses a "minilid" domain consisting of 5 amino acid residues instead of 23 in HPL (*24*).

In CoPLRP2, a full-length lid domain is present and the reason colipase has no effects in the presence of supramicellar bile salt concentrations is not clear. Almost all the residues involved in the interaction with colipase are conserved in both the C-terminal domain and the lid (*23*). One striking exception, however, is residue 403, which is conserved in the form of a tyrosine in all the classical lipases but differs in all the RP2 lipases. As mentioned previously, Y403 interacts with colipase via several van der Waals contacts in the HPL−colipase complex (*7*, *13*), and it was suggested that the point mutation of residue 403 in CoPLRP2 might lead to a lower affinity for colipase (*23*). Another hypothesis was that the lid domain of CoPLRP2 may possess a higher degree of freedom and that the interactions between the lid and colipase were weakened if not completely abolished. This hypothesis resulted from the finding that the interactions stabilizing the open conformation of the lid domain in HPL cannot exist in CoPLRP2 or in some other members of the PLRP2 subfamily (Figure 2). In HPL, the open lid domain interacts with the core of the protein via a salt bridge (D257−K268) and a hydrogen bond (R256−Y267). In the PLRP2 subfamily, these residues are almost all different, whereas they are completely conserved in the classical pancreatic lipases.

The finding that colipase had no effects on GPLRP2 and CoPLRP2 was initially taken to be a general characteristic of PLRP2s (*21*), but this idea was subsequently challenged by Jennens and Lowe (*25*) in the case of the rat PLRP2, which has also been named GP-3. Colipase was found to increase the lipase activity of GP-3 on tributyrin, trioctanoin, and triolein. The effects of colipase were not, however, as clear-cut as in the case of the classical pancreatic lipase, since the lipase activity of GP-3 was not inhibited by bile salts in the absence of colipase (*25*).

In the present study, we investigated whether the five mutations of residues 256, 257, 267, 268, and 403 might be responsible for the lack of the colipase effects observed in some PLRP2s. We produced and characterized three HPL

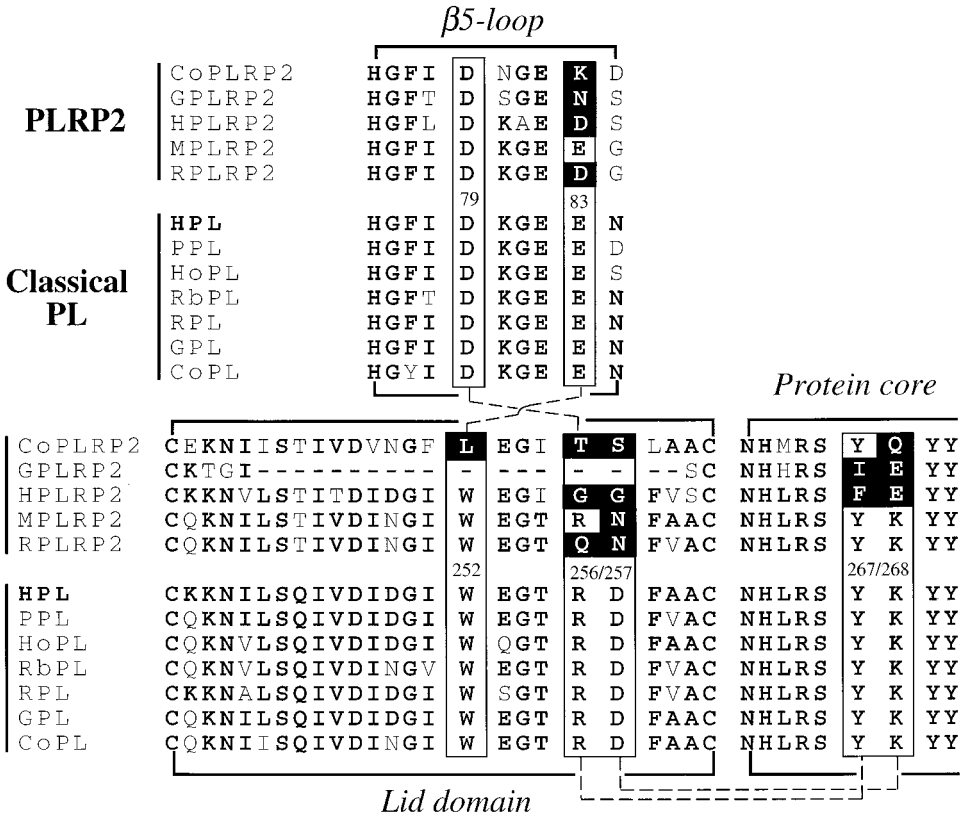

FIGURE 2: Interactions stabilizing the open conformation of the lid domain. A partial alignment of the amino acid sequence (β5 loop and lid domain) of classical pancreatic lipases and PLRP2 is shown. The results of the X-ray crystallographic study of the HPL−colipase−mixed micelle complex (*8*) showed that the open lid domain interacts with the core of the protein via a salt bridge (D257−K268) and a hydrogen bond (R256−Y267). In the PLRP2 subfamily, these residues are almost all different, whereas they are completely conserved in classical pancreatic lipases. The lid domain also interacts with the β5 loop via a salt bridge (R256−D79) and a hydrogen bond (W252−E83). Here again, most of these residues are different in the PLRP2 subfamily.

mutants: HPL Y403N, a HPL four-site mutant (R256G, D257G, Y267F, and K268E), and a HPL five-site mutant (R256G, D257G, Y267F, K268E, and Y403N), in which the HPL amino acids were replaced by those present in human PLRP2 at the same positions (*20*). The three mutants were expressed in insect cells and purified to homogeneity prior to being characterized with trioctanoin emulsions as the substrate. The inhibition by bile salts, the colipase dependence, and the interfacial binding of the three mutants were measured and compared to those of an HPL mutant [HPL-(−lid)] possessing a large deletion within the lid domain (*26*) and hence only one site of interaction with colipase.

MATERIALS AND METHODS

DNA Source and Manipulations. The cDNA encoding HPL was obtained from human placenta mRNA by PCR technology based on the complete sequence of HPL, including the leader sequence (*27*). A 1411 bp *Bam*HI DNA fragment containing the entire HPL coding region was subcloned into the *Bam*HI site of the pVL1392 vector (Invitrogen). A *Bam*HI/*Xho*I DNA fragment including HPL cDNA was also subcloned into the pIC19R vector (*28*). All plasmids were produced and amplified in *Escherichia coli* after electroporation of ElectroMAX DH10B cells (Life Technologies). Plasmid DNAs were isolated from *E. coli* cultures by the alkaline lysis procedure (*29*) and purified by use of the Wizard DNA purification system (Promega). Digestion with restriction enzymes and ligation with T4 DNA ligase were performed as recommended by the enzyme supplier (New England Biolabs). DNA sequencing was performed by means of the dideoxynucleotide chain-termination method (*30*) with the Sequenase version 2.0 DNA sequencing kit (Amersham Life Sciences).

Site-Directed Mutagenesis. Point mutations were performed by the PCR overlap extension technique (*26, 31*) with internal oligonucleotides carrying the specific mutations and two external oligonucleotides corresponding to the 5′ and 3′ ends of HPL cDNA, respectively. PCR reactions were carried out with *Pfu* DNA polymerase (Stratagene).

(A) HPL Y403N Mutant. The first PCR reaction was carried out with HPL cDNA in pVL1392 as the template and primers 1 and 4 (Table 1), for 30 cycles of 1 min at 94 °C, 2 min at 50 °C, and 3 min at 72 °C. The second PCR reaction was carried out with HPL cDNA in pVL1392 as the template and primers 2 and 3 (Table 1), for 30 cycles of 1 min at 94 °C, 2 min at 50 °C, and 3 min at 72 °C. The third PCR ligation−amplification step was carried out with the products of PCR 1 and PCR 2 as the templates, and primers 1 and 2 for 30 cycles of 1 min at 94 °C, 2 min at 50 °C, and 3 min at 72 °C. To check the mutation, a new *Nde*I restriction site was introduced into HPL cDNA by primers 3 and 4. The PCR3 product was digested by *Xho*I, and the resulting *Xho*I/*Xho*I DNA fragment (584 bp) containing the mutation was substituted for the homologous fragment in the pIC19R vector containing the original HPL cDNA. Several clones were screened to check that the *Xho*I/*Xho*I insert was properly oriented, and one of them was further sequenced to check that only the desired mutation was

Table 1: Primers Used for PCR Mutagenesis[a]

no.	primer sequences and comments
1	CCC ACA GGG GGA TCC GCT CGG CAT, sense primer annealing to HPL cDNA 5′ end, *Bam*HI
2	GGA TCA CTC GAG TCA GCA GGG TGT, antisense primer annealing to HPL cDNA 3′ end, *Xho*I
3	AAA TT**C** ATA TGG **A**AT AAC AAT GTG ATC, sense primer corresponding to the peptide KFIW**N**NNVI and encoding the Y403N mutation, *Nde*I
4	GTT AT**T** CCA **T**AT **G**AA TTT AAC CAT CTG, antisense primer corresponding to the peptide QMVKFIW**N**N and encoding the Y403N mutation, *Nde*I
5	GAA GGG ACT **G**GA G**G**C TTT GCG GCC TGT AAT CAC TTA AGA AGC T**T**C **G**AA TAT TAC ACT GAT, sense primer corresponding to the peptide EGT**GG**FAACNHLRS**FE**YYTD and encoding the R256G, D257G, Y267F, and K268E mutations, *Bst*BI
6	AGT GTA ATA TT**C** G**A**A GCT TCT TAA GTG ATT ACA GGC CGC AAA G**C**C TC**C** AGT CCC TTC CCA, antisense primer corresponding to the peptide WEGT**GG**FAACNHLRS**FE**YYT and encoding the R256G, D257G, Y267F, and K268E mutations, *Bst*BI
7	C ATT GGC CAC **G**GC CTG GGT GC, sense primer corresponding to the peptide IGH**G**LGA and encoding the S152G mutation
8	GC ACC CAG GC**C** GTG GCC AAT G, antisense primer corresponding to the peptide IGH**G**LGA and encoding the S152G mutation

[a] Point mutations are shown in boldface type. Restriction sites are underlined.

introduced by PCR. From the latter clone in pIC19R, an *Eco*RI/*Bgl*II DNA fragment including the entire coding sequence was subcloned into the pVL1393 baculovirus transfer vector.

(B) HPL Four-Site Mutant (R256G, D257G, Y267F, and K268E). The first PCR reaction was carried out with HPL cDNA in pVL1392 as the template and primers 1 and 6 (Table 1) for 30 cycles of 1 min at 94 °C, 2 min at 50 °C, and 3 min at 72 °C. The second PCR reaction was carried out with HPL cDNA in pVL1392 as the template and primers 2 and 5 (Table 1) for 30 cycles of 1 min at 94 °C, 2 min at 50 °C, and 3 min at 72 °C. The third PCR ligation−amplification step was carried out with the products of PCR 1 and PCR 2 as the templates and primers 1 and 2 for 30 cycles of 1 min at 94 °C, 2 min at 50 °C, and 3 min at 72 °C. To check the mutation, a new *Bst*BI restriction site was introduced into HPL cDNA by primers 5 and 6. A *Bam*HI/*Xho*I DNA fragment (1411 bp) from the PCR 3 product was cloned into the pIC19R vector for sequencing and introduction of new restriction sites (*Sma*I, *Bgl*II) at the cDNA 5′ and 3′ends, respectively. After the digestion by endonucleases, the *Sma*I/*Bgl*II DNA fragment (1420 bp) was further subcloned into the pVL1393 baculovirus transfer vector.

(C) HPL 5-Site Mutant (R256G, D257G, Y267F, K268E, Y403N). From the pIC19R vector containing the cDNA of the HPL Y403N mutant, an *Xba*I/*Bgl*II DNA fragment (373 bp) containing the single mutation was substituted for the corresponding fragment of the HPL four-site mutant (R256G, D257G, Y267F, and K268E) in pVL1393.

(D) HPL S152G Mutant. The first PCR reaction was carried out with HPL cDNA in pVL1392 as the template and primers 1 and 8 (Table 1) for 30 cycles of 1 min at 94 °C, 2 min at 55 °C, and 3 min at 72 °C. The second PCR reaction was carried out with HPL cDNA in pVL1392 as the template and primers 2 and 7 (Table 1) for 30 cycles of 1 min at 94 °C, 2 min at 55 °C, and 3 min at 72 °C. The third PCR ligation-amplification step was carried out with the products of PCR 1 and PCR 2 as templates and primers 1 and 2 for 30 cycles of 1 min at 94 °C, 2 min at 50 °C, and 3 min at 72 °C. The PCR 3 product was digested by *Nco*I and *Spe*I, and the resulting *Nco*I/*Spe*I DNA fragment (1022 bp) containing the mutation was substituted for the homologous fragment in the pVL1392 vector containing the original HPL cDNA.

Production of HPL Mutants in the Baculovirus Expression System. Recombinant baculovirus production and HPL mutant expression were performed as previously described (*26*, *32*). The pVL1393 baculovirus tranfer vectors containing the mutated HPL cDNAs were used for the cotransfection of Sf9 insect cells (*Spodoptera frugiperda*) with the linearized genomic DNA from *Autographa californica* baculovirus (AcMNPV from the BaculoGold transfection Kit, Pharmingen). The Sf9 cells were grown in monoloyers at 27 °C in tissue culture flasks, using TNM-FH medium (Sigma) supplemented with 10% fetal calf serum (Bio-Whittaker) and 1% of an antibiotic−antimycotic solution (Gibco BRL−Life Technologies) containing 10 000 units/mL penicillin G, 10 000 μg/mL streptomycin, and 25 μg/mL amphotericin B (Fungizone). With each mutant, the insect cell cotransfection was performed with 1 μg of linear AcMNPV DNA and 3 μg of the recombinant pVL1393 mixed with cationic liposomes and added to a 60 mm Petri dish containing 2×10^6 Sf9 cells grown in TNM-FH medium. The culture supernatants were collected after the lysis of all the cells (approximately 7 days postinfection) and were used as the primary stocks of the recombinant baculoviruses expressing HPL mutants. An additional stage of cell infection was performed to amplify the viruses and generate the high-titer virus stocks (10^7-10^9 plaque-forming units (pfu)/mL of culture) required for the recombinant protein production. The virus titers were estimated by the end-point dilution assay method as previously described (*33*). The production of the HPL mutants was carried out with another cell line from *Trichoplusia ni*, grown in a monolayer up to 5×10^7 cells/175 cm^2 culture flask, in 25 mL of EX-CELL 400 medium (Valbiotech) supplemented with 0.5% of the previously mentioned antibiotic−antimycotic solution. An inoculum of each recombinant baculovirus encoding an HPL mutant was added to the cell culture at a multiplicity of infection of around 10 pfu/cell. Six hours postinfection, the culture supernatant was removed by aspiration and replaced by 25 mL of fresh EX-CELL 400 medium. The baculovirus-infected insect cell cultures were harvested 3 days after the infection in order to prevent any intracellular proteases released upon cell lysis from degrading the recombinant protein.

Purification of HPL Mutants. The HPL mutants were purified by the one-step procedure previously developed for the purification of HPL expressed in insect cells (*32*). With each mutant, the culture medium was centrifuged at 10 000 rpm for 10 min and the supernatant was lyophilyzed for 24 h. The dry material was dissolved in a few milliliters of distilled water and dialyzed overnight against 10 mM MES buffer, pH 6.5. Prior to chromatography, the solution was

run through a 0.8 μm Millipore filter. By FPLC (Pharmacia), cation-exchange chromatography was performed on a Mono S HR 5/5 column equilibrated in 10 mM MES buffer, pH 6.5. After injection of each sample, a linear NaCl concentration gradient was applied from 0 to 100 mM NaCl, within 60 min. The flow rate was adjusted to 1 mL/min. The protein elution profile was recorded spectrophotometrically at 280 nm and the lipase activity was measured potentiometrically in all the fractions collected by the pH-stat technique with tributyrin as the substrate (see Lipase Activity Measurements section). The main fractions containing lipase activity were subjected to SDS−12% PAGE analysis (*34*), and those displaying a single protein band at 50 kDa were pooled and concentrated. The protein concentrations were estimated by performing amino acid analysis as well as a specific HPL ELISA (see ELISA for Measuring HPL S152G Concentrations section).

N-Terminal Amino Acid Sequencing. To check that the cleavage of HPL signal peptide had occurred appropriately, and to ensure that no proteolytic degradation had taken place, samples of the purified HPL mutants were subjected to automated Edman degradation using an Applied Biosystems Model 473 A gas-phase sequencer. The resulting phenylthiohydantoins were identified by performing HPLC on a C-18 Brownlee column (5 μm, 2.1 mm × 220 mm).

Mass Determination. The HPL mutants were analyzed by electrospray mass spectrometry (ESMS) on an API III LC/MS/MS system (Perkin-Elmer Sciex Instruments, Thornhill, Canada) as described previously in the case of the recombinant HPL (*32*).

Lipase Activity Measurements. The lipase activity of the HPL mutants was assayed in bulk by measuring the release of free fatty acids from mechanically stirred emulsions of either tributyrin or trioctanoin (puriss grade from Fluka). By use of a pH-stat (TTT 80 Radiometer, Copenhagen, Denmark), the free fatty acids were automatically titrated with 0.1 N NaOH at a constant pH value of 7.5. Each reaction was performed in a thermostated vessel (37 °C) containing 0.5 mL of substrate and 14.5 mL of 0.28 mM Tris-HCl buffer, 150 mM NaCl, and 1.4 mM $CaCl_2$, as well as a variable concentration of sodium taurodeoxycholate (NaTDC). When required, pure colipase from porcine pancreas was added at a molar excess of 5. The lipolytic activities are expressed here in international units (IU)/mg of enzyme. One unit corresponds to 1 μmol of fatty acid released per minute.

Binding of HPL and HPL Mutants to Trioctanoin Emulsions. The interfacial binding of HPL was assayed by mixing the enzyme with a trioctanoin emulsion formed in a pH-stat vial and by further measuring the lipase activity remaining in the water phase after the separation of the oil phase. A similar procedure was first described by Borgström, using tributyrin emulsions that were separated from the water phase by low-speed centrifugation (1200 rpm) for short periods of time (10 min) (*1*). With trioctanoin, it was difficult to achieve complete phase separation at low speeds and short periods of centrifugation. A gradient of oil droplets was observed, the size of which increased toward the upper end of the centrifuge tube. The droplets coalesced at the surface, where a pure oil phase formed. A clear isotropic water phase was obtained only at high speeds and/or long centrifugation times, and a complete coalescence of the oil occurred. Since a drastic decrease in the specific surface might favor the lipase desorption from the oil−water interface, gum arabic was added to stabilize the emulsion and a simple decantation was performed instead of centrifugation, to reduce the coalescence. The highest concentration that could be used without affecting HPL activity on trioctanoin was 0.4% (w/v) gum arabic.

The final binding assay was performed as follows: a pH-stat vial thermostated at 37 °C was filled with 500 μL of trioctanoin (puriss grade from Fluka) and 14.5 mL of 0.28 mM Tris-HCl buffer, 150 mM NaCl, 1.4 mM $CaCl_2$, and 0.4% gum arabic, containing either 0.5 or 4 mM NaTDC. The vial was placed on the automatic titrator (TTT 80 Radiometer, Copenhagen, Denmark) and its contents were stirred mechanically for 5 min in order to obtain a fine trioctanoin emulsion and to monitor the pH value at 7.5 by addition of 0.1 N NaOH. When required, colipase at a molar excess of 5 (10 μg, 1000 pmol) was added during this 5-min period. The lipase (10 μg of HPL, 200 pmol) was then added to the emulsion, and after 2 min of incubation, the contents of the pH-stat vial were transferred into a puncturable 25 × 64 mm centrifuge tube (Beckman Ultra-Clear), which was kept on the bench for 1 h in order to obtain a satisfactory phase separation. After creaming, the oil droplets accumulated at the top of the tube and a clear sample (1−2 mL) of the aqueous phase was recovered by introducing a 0.8 × 40 mm needle equipped with a 5-mL syringe into the bottom of the tube. The amount of lipase remaining in solution was determined by measuring the residual lipase activity from an aliquot of this clear aqueous phase with tributyrin as the substrate, with colipase in excess, as well as the lipase assay buffer required to obtain a final reaction volume of 15 mL. NaTDC was added to the assay buffer so that its final concentration in the 15-mL sample/buffer mixture was 0.5 mM and the maximum specific activity of HPL was reached [12 500 IU/mg (*32*)].

Similar experiments were carried out with several HPL mutants (HPL S152G, 10 μg; HPL(−lid), 40 μg; HPL four-site mutant, 50 μg) and a colipase molar excess of 5. The amounts of the mutants remaining in solution were estimated by ELISA in the case of HPL S152G (see below) or by measuring the residual lipase activity in the case of HPL-(−lid) and HPL four-site mutant. The two latter mutants were both assayed with trioctanoin as the substrate (specific activities 550 and 500 IU/mg, respectively, at 0.5 mM NaTDC).

Before each experiment, the pH-stat vial was washed successively with acetone, ethanol, and Milli-Q water in order to remove any trace of surface-active compound that might modify the emulsion stability.

ELISA for Measuring HPL S152G Concentrations. A double sandwich ELISA was performed to measure the amount of HPL S152G remaining in the aqueous phase during the interfacial binding experiments. Rabbit anti-HPL polyclonal antibodies (pAb) were purified as described by Aoubala et al. (*35*) and used as capture antibodies. The detector antibody was a mouse anti-HPL monoclonal antibody (mAb 146-40), which was produced and biotin-labeled as previously described (*35*, *36*). Each well of a 96-well microtitration plate was filled with 50 μL of anti-HPL pAb solution at 5 μg/mL (250 ng/well). The plate was kept at 4 °C overnight and washed twice with PBS (phosphate-buffered saline; 10 mM Na_2HPO_4/KH_2PO_4 and 150 mM

NaCl, pH 7.4) containing 0.05% (v/v) Tween 20 (washing buffer). Each well was then filled with 200 μL of PBS containing 3% (w/v) nonfat dry milk (saturating buffer). The plate was incubated at 37 °C for 2 h and washed 3 times for 5 min with the washing buffer. After saturation and washing, 50 μL of standard HPL solutions, ranging from 0 to 10 ng/mL, were added to the first 8-well row of the plate, whereas similar standard HPL S152G solutions were added to the second row. The other rows were filled with HPL S152G samples at various dilutions (1/100 to 1/800). The plate was incubated at 37 °C for 1 h and washed 3 times for 5 min with the washing buffer. Each well was then filled with 50 μL of anti-HPL mAb 146-40 biotin conjugate at 0.25 μg/mL (12.5 ng/well). The plate was incubated at 37 °C for 1 h and washed 3 times for 5 min with the washing buffer. Each well was then filled with 50 μL of streptavidin−peroxidase (Sigma) diluted with washing buffer at 1/1000. The plate was incubated at 37 °C for 45 min and washed 3 times for 5 min with the washing buffer. Each well was then filled with 50 μL of the peroxidase substrate solution (*o*-phenylenediamine from Sigma) and the plate was kept in the dark at room temperature for 15 min. The reaction was stopped by adding 50 μL of 0.5 M H_2SO_4, and the optical density at 492 nm was measured immediately with a MR5000 Dynatech spectrophotometer.

Protein Blotting/Protein Overlay Immunoassay. Porcine procolipase (20 μg) was dot-blotted on a PVDF membrane. The membrane was incubated for 1 h at room temperature with PBS (see the ELISA protocol above) containing 0.05% (v/v) Tween 20 and 3% (w/v) BSA. The saturated membrane was incubated for 2 h at room temperature with 0.28 mM Tris-HCl buffer, pH 7.5, 150 mM NaCl, 1.4 mM $CaCl_2$, and 4 mM NaTDC, containing either 1 μM HPL or HPL mutants. The membrane was further washed with the same Tris-HCl buffer and the immunodetection of the lipase−colipase complex was performed with an anti-HPL polyclonal antibody as previously described (*37*).

Monolayer Experiments. By use of the monolayer technique, the kinetics of the adsorption of HPL and HPL(−lid) were studied by recording the changes with time in the surface pressure of a monomolecular film of egg phosphatidylcholine (PC) spread at the air−water interface in a cylindrical Teflon trough (volume 5 mL, surface area 7 cm^2). The surface pressure was measured by the Wilhelmy method with a thin platinum plate (perimeter 3.94 cm) attached to an electromicrobalance (Beckman LM 600). The trough was filled with 10 mM Tris-HCl buffer (pH 8.0), 100 mM NaCl, 21 mM $CaCl_2$, and 1 mM EDTA, and the monolayer was spread with various volumes (1−10 μL) of a 1 mg/mL PC solution in chloroform. Once the initial surface pressure had stabilized, the lipase (5 μg) ± colipase (1 μg) was injected into the aqueous subphase, which was stirred for 30 s at 250 rpm with a magnetic rod in order to homogenize the aqueous phase. The increase in the surface pressure was then recorded for 60 min. To study the effects of colipase on the lipase adsorption, lipase and colipase were premixed at a 1:1 molar ratio before being injected into the aqueous subphase. We checked that sequentially injecting colipase first and lipase second yielded similar results.

Modeling of HPL(−lid) and Calculating the Water Accessible Surfaces. By use of the Turbo-Frodo software program (*38*), a 3D model of the HPL(−lid) mutant was constructed by superimposing the open 3D structure of HPL (*8*) on the 3D structure of the N-GPLRP2/C-HPL chimera (*10*). Both structures belong to the α/β hydrolase fold family (*39*) and are very similar, except that the chimera possesses an identical short lid domain (C237-K-T-G-I-S-C) to that introduced into HPL(−lid), instead of the large-sized lid domain that exists in HPL (*26*). Starting from the open 3D structure of HPL as the template, 18 residues (240−257) were deleted from the lid domain, and the Cα atoms from the remaining lid residues (C237-K238-K239/F258-A259-A260-C261) were fitted by torsion onto the Cα atoms of the minilid of the N-GPLRP2/C-HPL chimera. We checked that the dihedral angle values of the new lid backbone fell within the Ramachandran plot and a new peptide bond was created between K239 and F258. Four side chains were then mutated (K239T, F258G, A259I, and A260S) and adjusted by torsion. The final model was obtained after local refinement of the lid stereochemistry. The water-accessible surface of the HPL(−lid) model was calculated by use of the DSSP option (*40*) in the Turbo-Frodo software program.

RESULTS

Design, Expression, Purification, and Structural Analysis of the HPL Mutants. To determine whether residues 256, 257, 267, 268, and 403 are directly or indirectly involved in the HPL−colipase interactions, three HPL mutants were designed: HPL Y403N, an HPL four-site mutant (R256G, D257G, Y267F, and K268E), and an HPL five-site mutant (R256G, D257G, Y267F, K268E, and Y403N). With HPL cDNA as the template, the three mutated DNA constructs were obtained by the PCR overlap extension method (*31*) and further subcloned into baculovirus expression vectors for production of the corresponding recombinant proteins in insect cells.

The three HPL mutants were secreted into the culture medium of insect cells with yields ranging from 10 to 40 mg of recombinant protein/L. Due to the fact that the insect cells were grown in a serum-free medium, each HPL mutant was the main protein present in the culture medium, as shown by SDS−12% PAGE analysis (data not shown). Each mutant was purified to homogeneity by a single step of cation-exchange chromatography as previously described in the case of the recombinant HPL (*32*) or other pancreatic lipase mutants (*26*).

After being purified, the HPL mutants were subjected to N-terminal amino acid sequence analysis, which confirmed that all three mutants were produced in their mature forms and that their HPL signal peptides were correctly cleaved. The first 15 amino acid residues in each sequence [KEV-(C)YERLG(C)FSDDS] were found to be identical to those of the mature HPL (*27*). In each case, the presence of a single amino acid sequence and the results of the mass spectrometry analysis (see below) ruled out the possibility that any proteolytic degradation of the recombinant protein migh have occurred.

The molecular mass of each mutant was determined experimentally by electrospray mass spectrometry (Table 2). In each case, the experimental mass was about 1000 Da greater than the theoretical mass of the polypeptides. A similar result was previously obtained with the recombinant HPL produced by insect cells (*32*), and it was observed that

Table 2: Mass Spectrometry Analysis[a] of HPL Mutants

mutant	polypeptide theoretical mass (Da)	experimental mass (Da)	deviation from theory (Da)
HPL Y403N	49 471	50 475 ± 10	1004
HPL tetramutant	49 348	50 372 ± 10	1024
HPL pentamutant	49 299	50 311 ± 10	1012

[a] Matrix-assisted laser desorption ionization spectrometry was performed.

a short glycan chain was linked to the single N-glycosylation site of HPL (N166). The molecular mass of this glycan chain (1038 Da) corresponded to two *N*-acetylglucosamine, three mannose, and one fucose residues, as determined by carbohydrate analysis. A short glycan chain of this kind is classically observed with recombinant proteins produced by insect cells (*41*).

Using PCR technology, we also produced an inactive HPL mutant (HPL S152G) in which the active-site serine residue was replaced by a glycine residue. This mutant was used as a control in the study on the binding of HPL to triglyceride emulsions. The choice of the S152G substitution was based on sequence comparisons between HPL and the nonenzymatic yolk proteins (YP2 and YP3) from *Drosophila melanogaster* (*42*). The HPL S152G mutant was expressed and purified under the experimental conditions previously described in the case of HPL (*32*).

To study more closely the role of the lid domain in the HPL−colipase interactions and the interfacial binding, we also produced the HPL(−lid) mutant, the expression and biochemical characterization of which were described in a previous study (*26*). This lid deletion mutant was obtained by replacing the full-length lid domain of HPL by the minilid domain of GPLRP2 (5 amino acid residues instead of 23 in HPL) (*24*). HPL(−lid) still displays a significant level of activity toward triglycerides and does not show any interfacial activation (*26*). Based on the 3D structures of the open HPL−colipase complex (*8*) and the GPLRP2−HPL chimera (*10*), a 3D model of HPL(−lid) was constructed and found to have an active site that was directly accessible to the solvent. The β5 loop of HPL(−lid) was modeled under the conformation yielding the oxyanion hole, which is observed in the 3D structures of both the open HPL and the GPLRP2−HPL chimera with a shortened lid domain (*10*). Due to the large deletion occurring within the lid domain, no interaction between the lid and the N-terminal end of colipase is possible. Several hydrophobic amino acid residues surrounding the active site, mainly within the β5 and β9 loops, are exposed to solvent, as in the case of the open structure of HPL (Table 3). The overall hydrophobic surface of the HPL(−lid) is smaller, however, than in the open HPL, due to the lid deletion (844 vs 1462 Å^2). Nevertheless, the hydrophilic/hydrophobic balance of HPL(−lid) was found to be intermediate between those of the open and the closed HPL (Table 3).

Effects of Bile Salts and Colipase on the Lipolytic Activity of HPL Mutants. The effects of sodium taurodeoxycholate (NaTDC) on the activity of HPL Y403N and HPL four-site and five-site mutants were investigated in the presence or absence of colipase, with trioctanoin as the substrate (Figure 3). As established previously in the case of HPL (Figure 3A), colipase also restored the catalytic activity of the bile salt-inhibited HPL Y403N mutant at high bile salt concentrations (Figure 3C), whereas no reactivation by colipase was observed with either the HPL four-site or five-site mutant (Figure 3B,D) at bile salt concentrations above the critical micellar concentration (1−2 mM). An important point worth mentioning is the 10-fold decrease in the maximum specific activities recorded with the HPL four-site and five-site mutants (around 600 IU/mg at 0.25−0.5 mM NaTDC + colipase) in comparison with those of HPL and HPL Y403N (6000−7000 IU/mg).

In similar experiments performed with tributyrin as the substrate (data not shown), a similar absence of the effects of colipase on the HPL four-site and five-site mutants was observed. The maximum specific activities recorded (400−600 IU/mg at 0.25−0.5 mM NaTDC + colipase) were 20 times lower than those recorded with HPL Y403N and HPL (10 500−12 500 IU/mg).

With trioctanoin as the substrate, a 10-fold decrease in the lipase activity was also observed with the HPL(−lid) mutant (Figure 3E) in comparison with HPL (Figure 3A). Addition of colipase was found to produce a partial reactivating effect (Figure 3E), contrary to what was observed with the HPL four-site and five-site mutants (Figure 3B,D). A similar reactivation of a minilid lipase by colipase was previously observed with the GPLRP2−HPL chimera (*26*).

Interfacial Binding of HPL and HPL Mutants on a Trioctanoin Emulsion. Like long-chain triglycerides, which are the natural substrates of pancreatic lipase, pure trioctanoin is completely insoluble in water. The products of trioctanoin lipolysis are partly soluble in water, however, and they do not remain at the oil−water interface upon lipolysis. As a consequence, one can expect the interfacial "quality" and hence, the lipase adsorption process to remain unchanged upon lipolysis until the specific surface (surface per volume unit) of the trioctanoin emulsion has been greatly reduced.

Interfacial binding experiments were performed with two different bile salt concentrations: 0.5 mM NaTDC, which is the optimum concentration for measuring HPL activity without any absolute requirement in colipase (Figure 3A), and 4 mM NaTDC, which completely inhibits HPL in the absence of colipase (Figure 3A). Similar conditions were used with the HPL mutants (see Figure 3). The lipase and the trioctanoin emulsion were incubated for 2 min in a pH-stat vial to monitor the initial lipolysis and to check the enzymatic activity, and then the mixture was transferred to a puncturable plastic tube for decantation. One hour later, after complete phase separation, a sample of the clear water phase was collected and the residual lipase activity remaining in solution was measured. By using the same procedure without the emulsion, we checked that the recovery rate of HPL from the solution (15 nM HPL) was 98.3% ± 6.4% within an 8-h period. The loss of HPL due to nonspecific adsorption onto the glass or plastic vials was therefore negligible.

The results obtained with HPL are shown in Figure 4. At 0.5 mM NaTDC, 25.8% ± 5.6% HPL remained in the water phase in the absence of colipase. The interfacial binding was almost complete (only 3.4% ± 1.1% HPL remaining in solution) when the colipase was added. At 4 mM NaTDC, a strong desorption of HPL from the interface was observed, since 87.6% ± 2.2% HPL was recovered in the water phase. The anchoring effects of colipase were also clearly observed, since only 9.0% ± 0.2% HPL remained in solution when

Table 3: Water-Accessible Surfaces[a] of the Surface Loops Surrounding the Active Site of HPL and HPL(−lid)[b]

	closed HPL	open HPL (+colipase)	HPL(−lid)
C	370 (β5) + 21 (β9) + 749 (lid) = 1140	110 (β5) + 29 (β9) + 400 (lid) = 539	186 (β5) + 24 (β9) + 237 (lid) = 447
S	157 (β5) + 159 (β9) + 388 (lid) = 704	115 (β5) + 264 (β9) + 141 (lid) = 520	125 (β5) + 259 (β9) + 239 (lid) = 623
H	57 (β5) + 246 (β9) + 497 (lid) = 800	154 (β5) + 545 (β9) + 763 (lid) = 1462	151 (β5) + 526 (β9) + 167 (lid) = 844
HLB	2.30	0.72	1.27

[a] Water-accessible surfaces are given in square angstroms. [b] Only the β5 loop (residues 75−84), β9 loop (residues 203−223) and the lid domain (residues 237−261) have been included in the calculations. The water-accessible surfaces of the open HPL have been calculated in the presence of colipase to take into account the interaction between the lid domain and colipase. The residue classes are indicated by the letters C (charged; R, D, E, H, and K), S (semipolar; Q, G, N, C, S, and T) and H (hydrophobic; A, F, I, L, M, P, V, W, and Y). HLB is the hydrophilic/lipophilic balance and is defined by the (C + S)/H ratio.

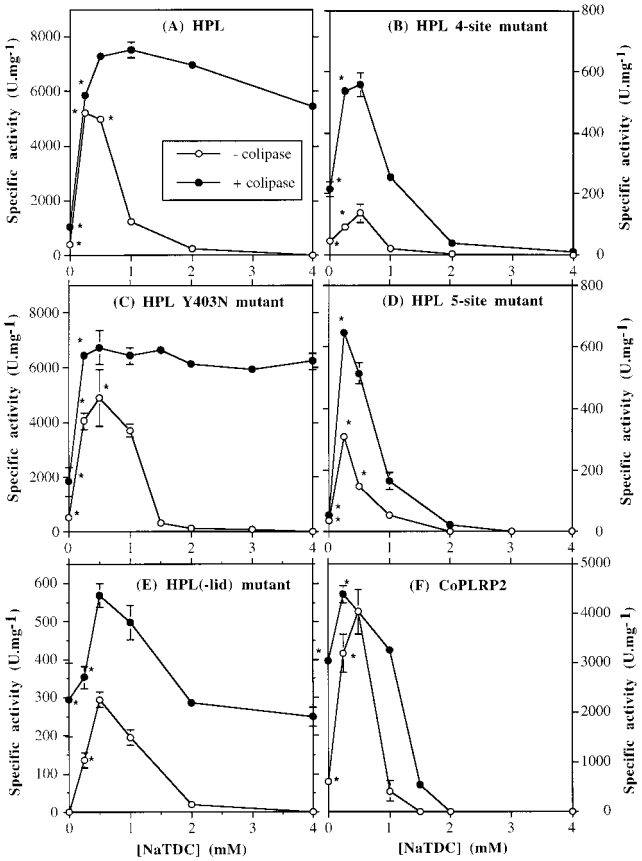

FIGURE 3: Effects of bile salts and colipase on the lipase activity of HPL, HPL mutants, and CoPLRP2 with trioctanoin as substrate. The asterisks give the lipolytic activities in terms of the initial velocities when the enzyme was inactivated at the interface during titration. At all the other points, the kinetics of fatty acid titration were found to be linear with time. When required, colipase was added at a molar excess of 5. Values are expressed as means ± SD (n = 3 for each experiment). Panels A and F were reprinted with permission from ref 21. Copyright 1994 American Chemical Society.

the colipase was added. A very strong correlation was therefore observed between the interfacial binding (Figure 4) and the lipase activity of HPL (Figure 3A).

To check the possibility that the lipolysis might affect the interfacial binding of HPL to trioctanoin, we also performed similar experiments with the inactive HPL S152G mutant, and its recovery from the water phase was estimated by ELISA. As shown in Figure 4, the interfacial binding behavior of HPL S152G was similar to that of the active HPL, which justified the use of our simple binding assay. In the case of the experiments with the active HPL, the lipolysis was probably largely reduced by the creaming of the emulsion, as well as by an acidification of the reaction mixture. A significant volume of the oil phase was still recovered after the 1-h phase separation period, confirming a partial lipolysis.

No significant differences were observed between HPL(−lid) and HPL (Figure 4), except at 0.5 mM NaTDC without colipase, where the interfacial binding of HPL(−lid) was slightly higher than that of HPL [13.9% ± 1.3% HPL(−lid) remaining in solution vs 25.8% ± 5.6% HPL].

The HPL four-site mutant was able to bind efficiently to the trioctanoin interface at 0.5 mM NaTDC, both with and without colipase (10.5% ± 0.9% and 7.8% ± 0.7% remaining in solution, respectively). The anchoring effects of colipase were, however, completely abolished at 4 mM NaTDC where 94.0% ± 1.2% HPL four-site mutant was still recovered from the water phase after the addition of colipase (Figure 4).

Lipase−Colipase Interactions. To check whether the HPL mutants were interacting with colipase in the presence of bile salts, we performed a set of experiments in which colipase was dot-blotted onto a PVDF membrane and was overlaid either by HPL or by each HPL mutant. The formation of the lipase−colipase complexes was further revealed by use of HPL polyclonal antibodies. HPL, HPL Y403N, and HPL four-site and five-site mutants, as well as HPL(−lid), were all found to bind colipase in the presence of 4 mM NaTDC (Figure 5). Similar results were obtained in the absence of bile salts (data not shown).

We performed a dose−response study of colipase addition with HPL Y403N, HPL(−lid), and HPL in order to estimate the apparent dissociation constants [$K_{D(app)}$] of the lipase−colipase complexes. Lipase activity measurements were carried out by the pH-stat technique with trioctanoin as substrate, in the presence of increasing amounts of colipase and 4 mM NaTDC, a bile salt concentration at which pancreatic lipase displays no activity in the absence of colipase. The lipase activity was then plotted as a function of the colipase to lipase molar ratio (Figure 6) and the $K_{D(app)}$ was calculated from a Scatchard curve as previously described by Rathelot et al. (*17*). It was assumed that the lipase activity was only resulting from a 1:1 molar association of lipase and colipase. As shown in Figure 6, colipase displayed a similar affinity for HPL and HPL(−lid), with $K_{D(app)}$ values of 1.5 ± 0.4 nM and 1.6 ± 0.3 nM, respectively. The colipase affinity for the HPL Y403N mutant was found to be reduced 3-fold, with a $K_{D(app)}$ of 4.9 ± 0.7 nM. Similar experiments with the HPL four-site and five-site mutants could not be performed since these mutants were not reactivated by colipase in the presence of 4 mM NaTDC.

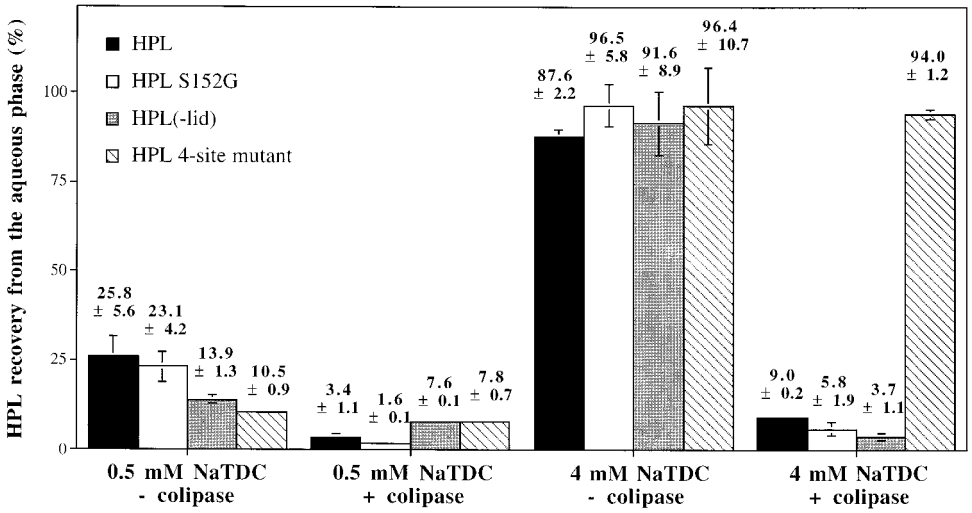

FIGURE 4: Effects of bile salts and colipase on the interfacial binding of HPL and HPL mutants to a trioctanoin emulsion. The interfacial binding experiments were performed at two different bile salt concentrations: 0.5 mM NaTDC, which is the optimum concentration for measuring HPL activity without any absolute colipase requirement, and 4 mM NaTDC, which completely inhibits HPL in the absence of colipase. When required, colipase was added at a molar excess of 5. Values are expressed as means ± SD ($n = 3$ for each experiment).

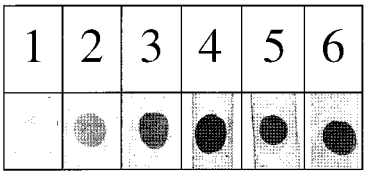

FIGURE 5: Binding of HPL and HPL mutants to colipase. Porcine colipase (20 μg) was dot-blotted on strips of PVDF membrane. The strips were then incubated with a 1 μM solution of either HPL (lane 2), HPL Y403N (lane 3), HPL four-site mutant (lane 4), HPL five-site mutant (lane 5), or HPL(−lid) (lane 6), in the presence of 4 mM NaTDC. Immunodetection of the lipase bound to colipase was performed with HPL polyclonal antibodies. A control experiment without lipase overlay is shown in lane 1.

Adsorption/Penetration of HPL and HPL(−lid) into a PC Monolayer, in the Presence or Absence of Colipase. Comparisons were made between HPL and HPL(−lid) surface properties by the monolayer technique, with monomolecular films of egg PC spread at the air−water interface. Egg PC is not a substrate for either HPL or HPL(−lid) (*26*), and the variations in the surface pressure recorded therefore reflect only the lipase adsorption/penetration into the lipid monolayer under which the lipase was injected. The maximum increase in the surface pressure ($\Delta\pi$) was plotted as a function of the initial surface pressure (π_i) of the egg PC monolayer (Figure 7). The critical surface pressure for penetration (π_c) was calculated for both HPL and HPL(−lid) from the linear curve fit of $\Delta\pi = f(\pi_i)$. π_c corresponds to the initial surface pressure beyond which no increase in the surface pressure occurs ($\Delta\pi = 0$) upon addition of the enzyme. The critical surface pressure for HPL(−lid) penetration ($\pi_c = 21.2$ mN/m) was found to be higher than that of HPL ($\pi_c = 14.9$ mN/m). HPL(−lid) can therefore be said to be a more penetrating enzyme than HPL. In the case of HPL, we checked that similar results were obtained with native HPL (nHPL), recombinant HPL (rHPL), and the inactive rHPL S152G mutant (Figure 7).

In the presence of porcine procolipase at a 1:1 molar ratio and for initial surface pressures ≤22 mN/m, the increase in the surface pressure after injection of the HPL−procolipase complex was higher than that observed after injection of procolipase or HPL alone. With the HPL(−lid)−procolipase complex, the increase in the surface pressure was higher than that observed after injection of HPL(−lid) alone, but it was not significantly different from that observed after injection of procolipase alone.

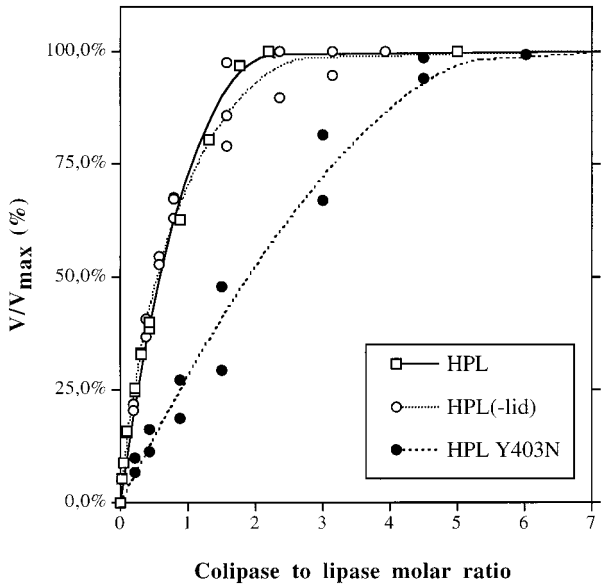

FIGURE 6: Effect of the colipase to lipase molar ratio on the enzymatic activity of HPL, HPL Y403N, and HPL(−lid). The lipase activity (ordinate) was expressed as the percent of the maximum lipase activity obtained with a large molar excess of colipase. The assays were performed by the pH-stat technique and trioctanoin as substrate (see Materials and Methods), in the presence of 4 mM NaTDC and increasing concentrations of porcine colipase. The lipase concentration in the pH-stat vial was 10 nM.

DISCUSSION

Mutations Affecting the Effects of Colipase on HPL. As previously reported by Jennens and Lowe (*43*), it was observed in the present study (Figure 3C) that the Y403N mutation in the HPL C-terminal domain did not affect the action of either bile salts or colipase at a 5-fold molar excess vs lipase, in comparison with what occurs in the case of HPL (Figure 3A). Y403 is therefore not essential to lipase−

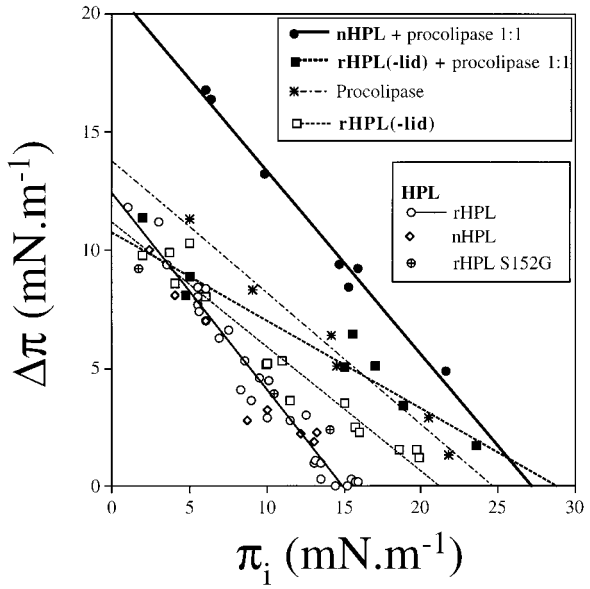

FIGURE 7: Adsorption of HPL and HPL(−lid) onto a monomolecular film of egg PC spread at the air−water interface. After injection of the enzyme ± procolipase into the subphase, the maximum increase in the surface pressure ($\Delta\pi$) was plotted as a function of the initial surface pressure (π_i) of the egg PC monolayer. Both $\Delta\pi$ and π_i are expressed in millinewtons per meter. The linear curves describing $\Delta\pi = f(\pi_i)$ were obtained by linear regression using the least-squares method. The corresponding equations are $\Delta\pi = -0.83\pi_i + 12.45$ ($R^2 = 0.961$) for HPL, $\Delta\pi = -0.53\pi_i + 11.19$ ($R^2 = 0.948$) for HPL(−lid), $\Delta\pi = -0.56\pi_i + 13.79$ ($R^2 = 0.98$) for procolipase alone, $\Delta\pi = -0.78\pi_i + 21.12$ ($R^2 = 0.987$) for HPL−procolipase complex 1:1, and $\Delta\pi = -0.37\pi_i + 10.74$ ($R^2 = 0.867$) for HPL(−lid)−procolipase complex 1:1. By use of these equations, the critical surface pressure for penetration (π_c, intercept with the π_i axis) was calculated for HPL (14.9 mN/m^{-1}), HPL(−lid) (21.2 mN/m^{-1}), procolipase alone (24.7 mN/m^{-1}), HPL−procolipase complex 1:1 (27.2 mN/m^{-1}), and HPL(−lid)−procolipase complex 1:1 (28.9 mN/m^{-1}). Abbreviations: rHPL, recombinant HPL produced in insect cells; nHPL, native HPL purified from human pancreatic juice.

colipase interactions, and the fact that colipase has no effect on some PLRP2s cannot be attributed to the systematic mutation of residue 403 in PLRP2s. We observed, however, that the Y403N mutation resulted in a lower affinity of HPL for colipase (Figure 6).

The lid domain needs to be open to bind colipase. In addition to the Y403N mutation, we also mutated four HPL amino acid residues (R256G, D257G, Y267F, and K268E) involved in the interactions stabilizing the open conformation of HPL (Figure 1). These four residues do not interact directly with colipase. As in the case of HPL (Figure 3A), the inhibition of the HPL four-site mutant lipase activity occurring at high bile salt concentration was due to the weak interfacial binding of the enzyme to the interface (Figure 4), but it was established that the interfacial anchoring effects of colipase are abolished when all four residues are mutated simultaneously.

Our results provide a potential explanation for the absence of any effects of colipase on CoPLRP2 at supramicellar bile salt concentrations (Figure 3F). Only three of the four residues are mutated in CoPLRP2 (Figure 2), but this is sufficient to abolish all the stabilizing interactions between the lid domain and the protein core.

In rat PLRP2, only two residues out of four are mutated (Figure 2) and colipase has been found to have activating effects (*25*). These data suggest that some interactions might subsist in RPLRP2 that stabilize the open lid conformation, although there can be no salt bridge (residue 257−residue 268) or hydrogen bond (residue 256−residue 267) between the lid domain and the protein core. It is worth noting, however, that RPLRP2 is the only characterized pancreatic lipase that is not inhibited by bile salts (*25*) and its kinetic properties therefore cannot be directly compared to those of CoPLRP2 or those of the HPL four-site mutant. Some other structural differences might exist in RPLRP2.

Role of the Lid Domain in HPL−Colipase Interactions and Interfacial Binding. Since no lid−colipase interactions can occur in the HPL(−lid) mutant due to the large deletion present within the lid domain, the C-terminal domain of HPL is the only lipase−colipase interaction site. Colipase did, however, have an effect on HPL(−lid): it restored the lipase activity at high bile salt concentrations (Figure 3E) and bound the enzyme at the interface of a trioctanoin emulsion (only 3.7% ± 1.1% HPL(−lid) remaining in solution at 4 mM NaTDC; Figure 4). Moreover, the apparent affinity of HPL(−lid) for colipase was found to be identical to that of HPL (Figure 6), and therefore, the contribution of the colipase−lid interactions (mainly three hydrogen bonds) is negligible as compared to the contribution of the colipase interactions with the HPL C-terminal domain (two salt bridges, six hydrogen bonds, several van der Waals contacts, and the apolar interaction between R65 from colipase and Y403 from lipase). In the absence of colipase and at low bile salt concentrations, the interfacial binding of HPL(−lid) was also very efficient. It is therefore concluded that the lid domain is not an essential element for either the interfacial binding of HPL or the productive lipase−colipase interaction required for the colipase to exert its anchoring effects.

Our results are at variance with those previously reported by Jennens and Lowe (*44*), who concluded that the lid domain was essential for HPL interfacial binding. These authors observed that two HPL lid deletion mutants (248−257 and 240−260, according to their numbering) did not bind efficiently to tributyrin in the absence of bile salts. In the presence of 4 mM NaTDC, the lipase activity and the interfacial binding to tributyrin of these mutants were very weak and increased only slightly upon adding colipase. The substrate was, however, different from our substrate, trioctanoin.

Using a phospholipid monomolecular film spread at the air−water interface, we also observed that HPL(−lid) is a more penetrating protein than HPL (Figure 7). Although these results were obtained with a completely different interface from the triglyceride−water interface, they also show that the lid domain is not essential to the interfacial binding. The adsorption/penetration capacity of HPL(−lid) is, however, not increased significantly by procolipase, on the contrary to what is observed with HPL (Figure 7) and what was reported earlier with porcine pancreatic lipase (*45*). In a recent study, however, Dahim and Brockman (*46*) have shown that the presence of colipase in the phospholipid monolayer did not enhance the pancreatic lipase adsorption and the surface pressure did not increase when the lipase was injected in the aqueous subphase at 18−20 mN/m. These results are at variance with our results: we observed (Figure 7) an increase of around 5 mN/m when HPL was injected under the phospholipid monolayer, after a preliminary injection of procolipase, at an initial surface pressure of 20

mN/m. We obtained the same result when lipase and procolipase were mixed before their injection in the aqueous subphase. Several differences in the experimental procedures might explain the apparent discrepancy between the two studies. In the case of the Dahim and Brockman experiments, the phospholipids and colipase were first mixed in a chloroform/methanol/water mixture before this mixture was spread onto the aqueous phase to form a mixed monolayer, a long-chain phospholipid was used, and procolipase was activated into colipase.

A Hypothesis Accounting for the Absence of the Anchoring Effects of Colipase on the HPL Four-Site Mutant. Since the lid domain is not essential for the lipase−colipase interactions, these interactions were presumably not abolished in the HPL four-site mutant. Using a protein blotting/protein overlay immunoassay, we demonstrated that colipase still binds to the HPL four-site mutant in the presence of bile salts (Figure 5). The fact that colipase had no anchoring effects on the HPL four-site mutant might result from a conformation of the lid domain preventing the interfacial binding of the lipase−colipase complex.

A similar hypothesis has been put forward by Lowe (*47*) in a study on the interactions between colipase and the open lid domain of HPL. After mutating a colipase residue (E15) interacting with N240 from the HPL lid, Lowe observed that the E15R colipase mutant was not able to reactivate HPL in the presence of bile salts, whereas this colipase mutant did reactivate HPL mutants in which the lid had been deleted. Lowe concluded that the E15R mutation in colipase generates a detrimental interaction with HPL that hinders the opening of the lid domain and that the deletion of the lid domain removes that hindrance, so that a functional interaction occurs between the E15R colipase and HPL. The study by Lowe indicates that the lid−colipase interactions contribute as much as the lid−HPL core interactions to stabilizing the open conformation of the lid and to producing a functional lipase−colipase complex.

Role of the Hydrophilic/Lipophilic Balance. In its closed conformation, HPL shows a high hydrophilic/lipophilic balance (HLB = 2.3; Table 3), which is consistent with its high solubility into water. When the lid opens, the HLB of HPL alone decreases considerably (0.72; Table 3) and HPL becomes an amphiphilic protein with a large hydrophobic surface exposed around its active site. The open HPL will then have a natural tendency to accumulate at interfaces but also to compete with other tensioactive molecules for adsorption onto these interfaces. As previously proposed by several authors (*1*, *4*, *48*−*51*), the inhibition of pancreatic lipase by bile salts might be due to bile salts having a higher affinity for the interface than that of HPL. In line with this hypothesis, the reversal of the bile salt inhibitory effects by colipase probably results from the reduction of the HLB in the open HPL−colipase complex. The association of HPL and colipase results in a larger hydrophobic surface being exposed on the same side of the complex.

Similar features are probably preserved in the HPL(−lid) mutant since its biochemical properties and those of HPL were found to be similar, except for the specific activities. The loops surrounding the active site of the HPL(−lid) model also showed a low HLB (1.27; Table 3).

In the HPL four-site mutant, the interactions stabilizing the open conformation of the lid domain are lost, and the equilibrium between the closed and open forms of HPL might shift toward the closed form. The HPL four-site mutant−colipase complex would then present a higher HLB and a lower affinity for the interface in the presence of bile salts.

Low Specific Activity of the HPL Lid Mutants. A common feature of the lid mutants produced in this study is their 10-fold lower specific activity in comparison with HPL (Figure 3). Based on the open 3D structures of the HPL−colipase complex, it has been established that several amino acid residues from the lid domain are involved in one of the acyl chain binding sites within the active center of HPL (*8*, *12*). This binding site does not exist in HPL(−lid), and the interaction between the substrate and the active site may be weakened. In the case of the HPL four-site mutant, it is possible that the removal of the interactions stabilizing the open conformation of the lid domain may also weaken the interactions between the lid domain and one acyl chain of the triglyceride substrate.

ACKNOWLEDGMENT

Our thanks are due to Daniel Campese (IBSM Marseille) for N-terminal sequence analysis, to Per F. Nielsen (Novo Nordisk A/S, Bagsvaerd, DK) for mass spectrometry analysis of the HPL mutants, to Dr. Alain de Caro for setting up the HPL ELISA, and to Dr. Jessica Blanc for revising the English. We are grateful to Professor Louis Sarda for his careful critical reading of the manuscript.

REFERENCES

1. Borgström, B. (1975) *J. Lipid Res. 16*, 411−417.
2. Momsen, W. E., and Brockman, H. L. (1976) *J. Biol. Chem. 251*, 378−383.
3. Borgström, B., and Erlanson, C. (1971) *Biochim. Biophys. Acta 242*, 509−513.
4. Borgström, B., and Erlanson-Albertsson, C. (1973) *Eur. J. Biochem. 37*, 60−68.
5. Vandermeers, A., Vandermeers-Piret, M. C., Rathé, J., and Christophe, J. (1974) *Biochim. Biophys. Acta 370*, 257−268.
6. Donner, J., Spink, C. H., Borgström, B., and Sjöholm, I. (1976) *Biochemistry 15*, 5413−5417.
7. van Tilbeurgh, H., Sarda, L., Verger, R., and Cambillau, C. (1992) *Nature 359*, 159−162.
8. van Tilbeurgh, H., Egloff, M.-P., Martinez, C., Rugani, N., Verger, R., and Cambillau, C. (1993) *Nature 362*, 814−820.
9. Breg, J. N., Sarda, L., Cozzone, P. J., Rugani, N., Boelens, R., and Kaptein, R. (1995) *Eur. J. Biochem. 227*, 663−672.
10. Withers-Martinez, C., Carrière, F., Verger, R., Bourgeois, D., and Cambillau, C. (1996) *Structure 4*, 1363−1374.
11. Hermoso, J., Pignol, D., Penel, S., Roth, M., Chapus, C., and Fontecilla-Camps, J. C. (1997) *EMBO J. 16*, 5531−5536.
12. Egloff, M.-P., Marguet, F., Buono, G., Verger, R., Cambillau, C., and van Tilbeurgh, H. (1995) *Biochemistry 34*, 2751−2762.
13. Egloff, M.-P., Sarda, L., Verger, R., Cambillau, C., and van Tilbeurgh, H. (1995) *Protein Sci. 4*, 44−57.
14. Patton, J. S., Albertsson, P. A., Erlanson, C., and Borgström, B. (1978) *J. Biol. Chem. 253*, 4195−4202.
15. Momsen, W. E., and Brockmann, H. L. (1976) *J. Biol. Chem. 251*, 384−388.
16. Patton, J. S., Donner, J., and Borgström, B. (1978) *Biochim. Biophys. Acta 529*, 67−78.
17. Rathelot, J., Julien, R., Bosc-Bierne, I., Gargouri, Y., Canioni, P., and Sarda, L. (1981) *Biochimie 63*, 227−234.
18. Sternby, B., and Erlanson-Albertsson, C. (1982) *Biochim. Biophys. Acta 711*, 193−195.
19. Verger, R. (1984) in *Lipases* (Borgström, B., and Brockman, H. L., Eds.) pp 83−149, Elsevier, Amsterdam.
20. Giller, T., Buchwald, P., Blum-Kaelin, D., and Hunziker, W. (1992) *J. Biol. Chem. 267*, 16509−16516.

21. Thirstrup, K., Verger, R., and Carrière, F. (1994) *Biochemistry 33*, 2748−2756.
22. De Caro, J., Carrière, F., Barboni, P., Giller, T., Verger, R., and de Caro, A. (1998) *Biochim. Biophys. Acta 1387*, 331−341.
23. Carrière, F., Thirstrup, K., Boel, E., Verger, R., and Thim, L. (1994) *Protein Eng. 7*, 563−569.
24. Hjorth, A., Carrière, F., Cudrey, C., Wöldike, H., Boel, E., Lawson, D. M., Ferrato, F., Cambillau, C., Dodson, G. G., Thim, L., and Verger, R. (1993) *Biochemistry 32*, 4702−4707.
25. Jennens, M. L., and Lowe, M. E. (1995) *J. Lipid Res. 36*, 2374−2382.
26. Carrière, F., Thirstrup, K., Hjorth, S., Ferrato, F., Withers-Martinez, C., Cambillau, C., Boel, E., Thim, L., and Verger, R. (1997) *Biochemistry 36*, 239−248.
27. Lowe, M. E., Rosenblum, J. L., and Strauss, A. W. (1989) *J. Biol. Chem. 264*, 20042−20048.
28. Marsh, J., L, Erfle, M., and Wykes, E., J. (1984) *Gene 32*, 481−485.
29. Sambrook, J., Fritsch, E. F., and Maniatis, T. (1989) *Molecular cloning. A laboratoty manual*, 2nd ed., Cold Spring Harbor Laboratory Press, Cold Spring Harbor, NY.
30. Sanger, F., Nicklen, S., and Coulson, A. R. (1977) *Proc. Natl. Acad. Sci. U.S.A. 74*, 5463−5467.
31. Higuchi, R. (1992) in *PCR Technology: Principles and Applications for DNA Amplification.* (Erlich, H. A., Ed.) pp 61−70, W. H. Freeman and Co., New York.
32. Thirstrup, K., Carrière, F., Hjorth, S., Rasmussen, P. B., Wöldike, H., Nielsen, P. F., and Thim, L. (1993) *FEBS Lett. 327*, 79−84.
33. O'Reilly, D. R., Miller, L. K., and Luckow, V. A. (1994) in *Baculovirus expression vectors: a laboratory manual*, pp 132−134, Oxford University Press, New York.
34. Laemmli, U. K. (1970) *Nature 227*, 680−685.
35. Aoubala, M., de la Fournière, L., Douchet, I., Abousalham, A., Daniel, C., Hirn, M., Gargouri, Y., Verger, R., and De Caro, A. (1995) *J. Biol. Chem 270*, 3932−3937.
36. Aoubala, M., Douchet, I., Bezzine, S., Hirn, M., Verger, R., and De Caro, A. (1997) in *Methods in Enzymology* (Dennis, E., and Rubin, B., Eds.) pp 126−149, Academic Press, Inc., San Diego, CA.
37. Bezzine, S., Carrière, F., De Caro, J., Verger, R., and De Caro, A. (1998) *Biochemistry 37*, 11846−11855.
38. Roussel, A., and Cambillau, C. (1989) in *Silicon Graphics Geometry Partners Directory*, pp 77−78, Silicon Graphics, Mountain View, CA.
39. Ollis, D. L., Cheah, E., Cygler, M., Dijkstra, B., Frolow, F., Franken, S. M., Harel, M., Remington, S. J., Silman, I., Schrag, J., Sussman, J. L., Verschueren, K. H. G., and Goldman, A. (1992) *Protein Eng. 5*, 197−211.
40. Kabsch, W., and Sander, C. (1983) *Biopolymers 22*, 2577−2637.
41. Aeed, P. A., and Elhammer, A. P. (1994) *Biochemistry 33*, 8793−8797.
42. Hide, W. A., Chan, L., and Li, W. H. (1992) *J. Lipid Res. 33*, 167−178.
43. Jennens, M. L., and Lowe, M. E. (1995) *J. Lipid Res. 36*, 1029−1036.
44. Jennens, M. L., and Lowe, M. E. (1994) *J. Biol. Chem. 269*, 25470−25474.
45. Verger, R., Rietsch, J., and Desnuelle, P. (1977) *J. Biol. Chem. 252*, 4319−4325.
46. Dahim, M., and Brockman, H. (1998) *Biochemistry 37*, 8369−8377.
47. Lowe, M. E. (1997) *J. Biol. Chem. 272*, 9−12.
48. Morgan, R. G. H., Barrowman, J., and Borgström, B. (1969) *Biochim. Biophys. Acta 175*, 65−75.
49. Brockerhoff, H. (1973) *Chem. Phys. Lipids 10*, 215−222.
50. Chapus, C., Sari, H., Sémériva, M., and Desnuelle, P. (1975) *FEBS Lett. 58*, 155−158.
51. Canioni, P., Julien, R., Rathelot, J., and Sarda, L. (1976) *Biochimie 58*, 751−753.

BI982601X